doi:10.1016/j.jmb.2007.02.031 J. Mol. Biol. (2007) 368, 1187–1201

JMB

Available online at www.sciencedirect.com

ScienceDirect

ELSEVIER

Biophysical Characterization of Structural Properties and Folding of Interleukin-1 Receptor Antagonist

Ramil F. Latypov[1]*, Timothy S. Harvey[2], Dingjiang Liu[3] Pavel V. Bondarenko[3], Tadahiko Kohno[4], Roger A. Fachini II[4] Robert D. Rosenfeld[4], Randal R. Ketchem[5], David N. Brems[3] and Andrei A. Raibekas[3]

[1]*Department of Pharmaceutics Amgen, Inc., 1201 Amgen Court West, Seattle WA 98119-3105, USA*

[2]*Department of Molecular Structure, Amgen, Inc. One Amgen Center Drive Thousand Oaks CA 91320-1799, USA*

[3]*Department of Pharmaceutics Amgen, Inc., One Amgen Center Drive, Thousand Oaks CA 91320-1799, USA*

[4]*Department of Protein Science Amgen, Inc., One Amgen Center Drive, Thousand Oaks CA 91320-1799, USA*

[5]*Department of Protein Science Amgen, Inc., 1201 Amgen Court West, Seattle WA 98119-3105, USA*

**Corresponding author*

Structural properties and folding of interleukin-1 receptor antagonist (IL-1ra), a therapeutically important cytokine with a symmetric β-trefoil topology, are characterized using optical spectroscopy, high-resolution NMR, and size-exclusion chromatography. Spectral contributions of two tryptophan residues, Trp17 and Trp120, present in the wild-type protein, have been determined from mutational analysis. Trp17 dominates the emission spectrum of IL-1ra, while Trp120 is quenched presumably by the nearby cysteine residues in both folded and unfolded states. The same Trp17 gives rise to two characteristic negative peaks in the aromatic CD. Urea denaturation of the wild-type protein is probed by measuring intrinsic and extrinsic (binding of 1-anilinonaphthalene-8-sulfonic acid) fluorescence, near- and far-UV CD, and 1D and 2D (^{1}H–^{15}N heteronuclear single quantum coherence (HSQC)) NMR. Overall, the data suggest an essentially two-state equilibrium denaturation mechanism with small, but detectable structural changes within the pretransition region. The majority of the ^{1}H–^{15}N HSQC cross-peaks of the folded state show only a limited chemical shift change as a function of the denaturant concentration. However, the amide cross-peak of Leu31 demonstrates a significant urea dependence that can be fitted to a two-state binding model with a dissociation constant of 0.95±0.04 M. This interaction has at least a five times higher affinity than reported values for nonspecific urea binding to denatured proteins and peptides, suggesting that the structural context around Leu31 stabilizes the protein–urea interaction. A possible role of denaturant binding in inducing the pretransition changes in IL-1ra is discussed. Urea unfolding of wild-type IL-1ra is sufficiently slow to enable HPLC separation of folded and unfolded states. Quantitative size-exclusion chromatography has provided a hydrodynamic view of the kinetic denaturation process. Thermodynamic stability and unfolding kinetics of IL-1ra resemble those of structurally and evolutionary close IL-1β, suggesting similarity of their free energy landscapes.

Keywords: protein folding; stability; denaturant binding; spectroscopy; NMR

Abbreviations used: ANS, 1-anilinonaphthalene-8-sulfonic acid; ESI, electrospray ionization; FGF, fibroblast growth factor; HA-HCl, hydroxylamine hydrochloride; HSQC, heteronuclear single-quantum coherence; IL-1ra, (human recombinant) interleukin-1 receptor antagonist; IL-1α, interleukin-1α; IL-1β, interleukin-1β; MS, mass spectrometry; NATA, *N*-acetyl-L-tryptophanamide; RP HPLC/MS, reversed-phase high performance liquid chromatography/mass spectrometry; T_m, melting temperature; WT, wild-type.

E-mail address of the corresponding author: rlatypov@amgen.com

Introduction

Since the discovery of proteins exhibiting a β-trefoil topology there has been substantial interest in understanding their folding mechanism.[1–15] The well-known interleukin-1β (IL-1β), fibroblast growth factor (FGF), and hisactophilin have less than 17% sequence identity, yet their folded structures are very similar.[1,16–22] In view of the critical role that native topology plays in protein folding,[23–25] the β-trefoil family offers a unique model for gaining insight into the interplay between long-range and short-range interactions in the formation of the native structure. Progress has been made in computational analysis of the various folding pathways related to the experimentally observed conformational transitions in β-trefoil proteins.[26] There is no doubt that characterization of other members of this family, such as interleukin-1 receptor antagonist (IL-1ra), will be beneficial for developing detailed computational descriptions of protein free energy landscapes and will promote understanding of the factors determining the existence of different folding pathways.

Insight into the relationship of protein structure, stability, and folding is also required for optimizing protein therapeutics toward higher potency, ease of delivery, and uncompromised long-term storage. IL-1ra is a therapeutically important cytokine and naturally occurring modulator of inflammatory and immune responses mediated by interleukin-1α (IL-1α) and IL-1β.[27,28] It acts as a receptor-binding antagonist that competes with IL-1α and IL-1β for the Type I IL-1 receptor, but does not elicit IL-1-associated responses. The amino acid sequence of IL-1ra is 26% identical to that of IL-1β[29] and its 3D structure has been determined by X-ray crystallography and NMR.[30–33] The high-resolution crystal structure of recombinant human IL-1ra is shown in Figure 1 (PDB ID: 1ILR[32]). Although the crystal form of the protein is an asymmetric dimer, IL-1ra is monomeric in solution, including the experimental conditions of this study. It is composed of 153 amino acid residues (including N-terminal methionine), is predominantly β-sheet, and exhibits a pseudo-3-fold symmetry characteristic of the β-trefoil fold.[1] In contrast to the single tryptophan containing IL-1β, IL-1ra has two tryptophan residues, Trp17 and Trp120, and two extra cysteine residues (for a total of four). Crystallographic data suggest that two of the cysteine residues, Cys70 and Cys117, can form a disulfide bond, while the other two residues, Cys67 and Cys123, are well separated in the folded structure.[32]

In our previous work, we characterized the aggregation properties of IL-1ra at high protein concentrations (>100 mg/mL) and elevated temperatures.[34] Aggregation of IL-1ra can be induced by nondenaturing temperatures (40–42 °C) and modulated by salt and specific anions, such as citrate and pyrophosphate. However, little was known about the conformational transitions and stability of IL-1ra at relatively low protein concentrations and ambient temperature. Here we attempted to gain an insight into the structural properties and folding of IL-1ra using urea as a denaturant. To this end, we have performed detailed characterization of equilibrium denaturation of the wild-type protein by optical spectroscopy and high-resolution NMR, as well as employed quantitative size-exclusion HPLC to study its unfolding kinetics. Further understanding of IL-1ra structural and optical properties has been gained by analyzing its single tryptophan variants, W17A and W120F. In the case of protein fluorescence and CD, the individual spectral contributions of the two tryptophan residues are very different. In addition, ^{1}H–^{15}N HSQC chemical peak shift analysis has revealed the existence of a relatively strong and specific protein–urea interaction in a well-defined cavity on the surface of IL-1ra.

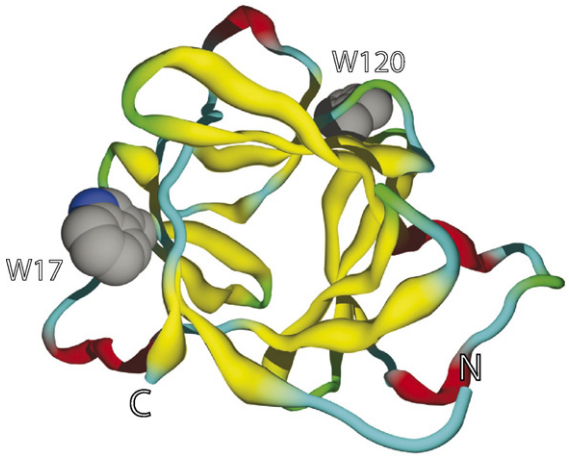

Figure 1. The asymmetric crystal unit of IL-1ra contains two independent protein molecules, molecule 1 and molecule 2 (PDB ID: 1ILR[32]). Presented here is a ribbon diagram of molecule 1. The secondary structural elements in the protein include 12 β-strands arranged into a β-trefoil architecture, short 3_{10} helices, and no α-helices. Color coding is as follows: yellow, β-strands; red, 3_{10} helices; green, β-turns; cyan, loops. The two distant tryptophan residues, Trp17 and Trp120, are explicitly shown. The N and C termini are indicated.

Results

Fluorescence and CD spectra of wild-type (WT) IL-1ra and its single tryptophan variants

Wild-type IL-1ra contains two tryptophan residues, Trp17 and Trp120, which are distant from each other within the protein molecule (C^{α}–C^{α} distance ~19 Å). Because their individual spectral properties were unknown, we constructed two single tryptophan variants, W17A and W120F, as described under Materials and Methods. The W120F substitution was expected to be tolerated by the protein structure because it is equivalent to the previously

studied mutant of structurally similar IL-1β.[35] Trp17 of IL-1ra was implicated in forming cation–π interactions stabilizing its crystal dimer[34,36,37] and the W17A substitution was chosen to eliminate aromaticity and hydrophobicity at this position. Emission spectra of the folded and urea unfolded states of the IL-1ra variants are shown in Figure 2(a). The signal intensities correspond to normalized values relative to equimolar *N*-acetyl-L-tryptophanamide (NATA) measured under identical conditions (gray dash–dot spectrum). In the absence of urea, the spectrum of the wild-type protein is very intense and red-shifted, with a maximum around 345 nm (black solid spectrum) characteristic of tryptophan residues in a polar environment.[38] The emission spectrum of urea-denatured protein has about 50% of the native state intensity and a maximum closer to 350 nm (black dashed spectrum). In addition, its spectrum shows a weak tyrosine emission around 300 nm, which is absent in the case of the folded protein. Replacement of Trp17 by an alanine results in about a 90% decrease in tryptophan fluorescence (red solid spectrum). In the folded state, W17A shows no defined tryptophan fluorescence maximum and its emission is dominated by the tyrosine band. Denaturation of W17A results in a small increase in tryptophan fluorescence with a maximum around 350 nm and a concomitant drop in tyrosine emission (red dashed spectrum). In contrast, folded W120F shows no tyrosine emission and its tryptophan fluorescence is lower than that of the wild-type protein by only 20% (blue solid spectrum). Similar to the wild-type protein, tryptophan fluorescence of denatured W120F is decreased by ~60% with only a small red shift (blue dashed spectrum) and at the same time its tyrosine fluorescence is increased.

Based on comparison of W120F with equimolar NATA, Trp17 is hyperfluorescent in the native state. To test whether this can be explained by a resonance energy transfer from tyrosine residues to Trp17, an experiment was performed with the excitation wavelength set to 300 nm. Trp17 shows hyperfluorescence irrespective of tyrosine excitation (data not shown).

Figure 2(b) shows near-UV CD spectra of the folded and unfolded states of the IL-1ra variants. In the absence of urea, the wild-type spectrum in the aromatic region (260–300 nm) has two pronounced negative peaks at 276 and 283 nm (black solid spectrum). Denaturation of IL-1ra in 6.5 M urea results in a loss of these peaks due to transition to a disordered conformation (black dashed spectrum). In contrast, the CD spectrum of folded W17A is devoid of the negative peaks (red solid spectrum), but distinct from the denatured state (red dashed spectrum) because it shows more positive ellipticity and has some residual fine structure. Quite the opposite, the spectrum of folded W120F is more intense and negative (blue solid spectrum) compared to that of wild-type IL-1ra. Beside the intensity difference, there is qualitative spectral correspondence between the W120F and wild-type

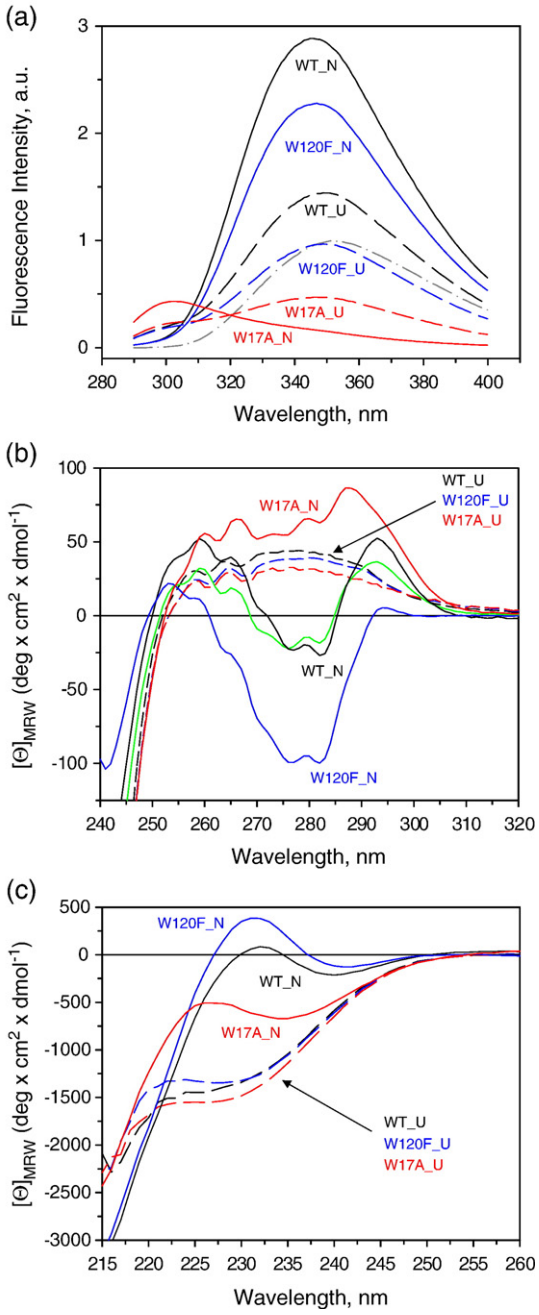

Figure 2. Spectra of the folded and unfolded (in 6.5 M urea) states of wild-type IL-1ra and its single tryptophan variants as measured by (a) fluorescence, (b) near-UV CD, and (c) far-UV CD. Solid and dashed black lines correspond to the folded and unfolded states of the wild-type protein, respectively. Solid and dashed red lines correspond to the folded and unfolded states of W17A, respectively. Solid and dashed blue lines correspond to the folded and unfolded states of W120F, respectively. The gray dash–dot spectrum in (a) corresponds to equimolar NATA measured under identical conditions. The green spectrum in (b) corresponds to the sum of the near-UV CD spectra of W17A and W120F (see text). Spectra of blank buffer solutions measured under matching conditions were used for background subtraction. The measurements were performed at 25 °C in 50 mM sodium phosphate, 5 mM DTT, 5 mM HA-HCl, pH 7.0. "N" and "U" in the protein names denote native and unfolded states, respectively.

spectra. And, as expected for unfolded conformations, there is no significant difference between the proteins in 6.5 M urea.

Figure 2(c) shows far-UV CD spectra of the folded and unfolded states of the IL-1ra variants. Spectral properties of wild-type IL-1ra are similar to that of other β-trefoil proteins, such as acidic FGF and IL-1β.[10,35,39] Denaturation of the protein is manifested by a pronounced spectral change around 230 nm and is seen as an increase in negative ellipticity from a near-zero value characteristic to the folded state (black solid spectrum). CD signal below 215 nm is also structurally informative, but is more difficult to use due to intrinsically small ellipticity changes and high background absorbance (data not shown). In the absence of urea, W17A (red solid spectrum) has spectral properties between those of wild-type folded and unfolded states, while its unfolded state spectrum (red dashed) is similar to that of the wild-type protein. In contrast, folded W120F has near wild-type spectral characteristics with somewhat more positive ellipticity (blue solid spectrum). Unfolding of W120F is seen as an increase in negative ellipticity (blue dashed spectrum) in accordance with the data for the wild-type protein and W17A.

Thermal denaturation of WT IL-1ra and its single tryptophan variants

To probe stability of the IL-1ra variants, their temperature denaturation profiles were recorded for the temperature range of 5–85 °C. Previously we showed that the wild-type protein can be reversibly heat denatured at low concentrations in the presence of salt.[34] Figure 3 illustrates thermal denaturation of the proteins monitored in the far-UV CD region at 230 nm. The ellipticity changes were measured for 5 μM protein solutions in 45 mM sodium phosphate

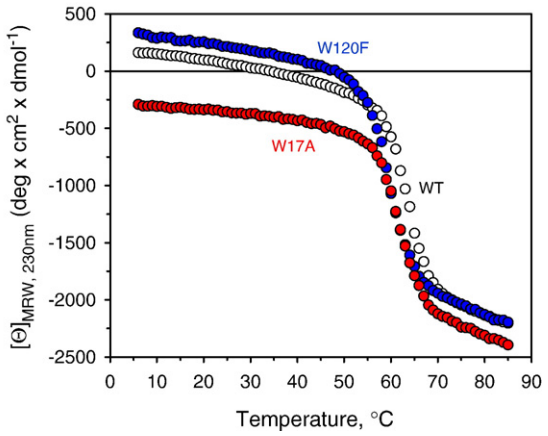

Figure 3. Temperature denaturation of the wild-type IL-1ra and its single tryptophan variants as measured by far-UV CD at 230 nm. Sample composition was as follows: 5 μM IL-1ra in 45 mM sodium phosphate (pH 7.0), 10% D_2O, 0.5 M NaCl. Open symbols correspond to the wild-type IL-1ra, red symbols correspond to W17A, and blue symbols correspond to W120F.

(pH 7.0) with 10% D_2O and 0.5 M NaCl (see Materials and Methods). In agreement with the spectral changes observed upon urea unfolding (see above), thermal denaturation of IL-1ra is manifested by an increase in negative ellipticity. There is a correspondence between native ellipticity values for the urea and thermal denaturation studies, while at high temperatures they seem to become more negative for heat-denatured proteins compared to the urea unfolded states (cf. Figures 2(c), 5(d), and 3). All variants show essentially linear temperature dependence up to 45 °C, followed by a sharp signal change between 55 and 70 °C. Above 70 °C all proteins are denatured and their ellipticity changes linearly with temperature. Based on the data, the proteins exhibit T_m values of ~63, ~62, and ~60 °C for the wild-type protein, W17A, and W120F, respectively.

Kinetic unfolding of WT IL-1ra characterized by CD and size-exclusion HPLC

In order to characterize the kinetic unfolding process of WT IL-1ra, native protein was manually mixed with a denaturing buffer to achieve an increase in urea concentration from 0 to 6.5 M. The kinetic process was followed overnight either at 230 or 283 nm at 25 °C to monitor changes in the backbone conformation and the tertiary structure. Fitting of a single-exponential equation to the data yielded rate constants of $7.08 \pm 0.03 \times 10^{-5}$ s^{-1} and $7.56 \pm 0.04 \times 10^{-5}$ s^{-1}, for the far- and near-UV CD, respectively (data not shown). In order to further characterize this slow unfolding reaction, we employed size-exclusion chromatography to separate and quantify compact and expanded conformations as a function of time. A typical size-exclusion HPLC run takes approximately 10 min (see Materials and Methods) and since its duration is about 20 times shorter than the interconversion time for CD-detected IL-1ra unfolding, a complete separation of folded and unfolded conformations can be achieved as illustrated in Figure 4. Snapshots of the kinetic process were obtained *via* multiple injections from a sample solution equilibrated at 25 °C. The first injection was made immediately after the protein was manually mixed with urea, and the corresponding chromatogram shows a single folded peak with a retention time of ~10.2 min. Protein unfolding is seen as a decrease in the area under the folded peak and a concomitant growth of the unfolded peak at ~8.4 min. The peaks are well separated, which facilitates their integration and quantitative analysis. Fitting of a single-exponential equation to the folded peak area as a function of time yielded a rate constant of $7.0 \pm 0.1 \times 10^{-5}$ s^{-1} (data not shown), which is close to the rate constants obtained from the CD measurements, confirming that all these techniques monitor global unfolding of the protein. Based on the kinetic results, equilibrium samples were pre-incubated overnight at the experimental temperature (25 °C) to achieve complete conformational equilibration prior to measurements.

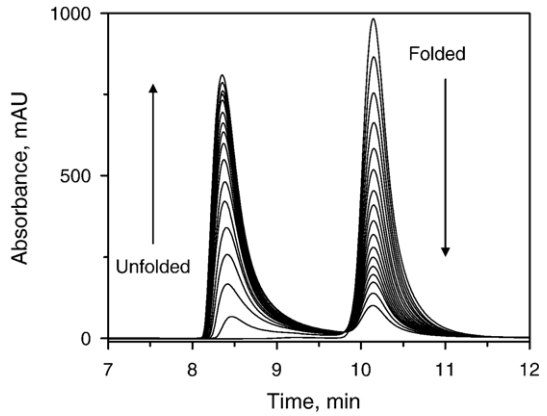

Figure 4. Size-exclusion HPLC profiles illustrating urea-induced unfolding process of WT IL-1ra at 25 °C. Experimental conditions: 50 mM sodium phosphate (pH 7.0), 5 mM DTT, 5 mM HA-HCl, 6.5 M urea.

Equilibrium unfolding of WT IL-1ra characterized by fluorescence and CD

Figure 5(a) shows equilibrium urea denaturation of WT IL-1ra measured at 303 and 350 nm using a T-format fluorimeter (see Materials and Methods). This approach allows simultaneous monitoring of changes in tyrosine and tryptophan fluorescence. In agreement with the data in Figure 2(a), unfolding of the protein results in ~50% decrease in the intensity of tryptophan emission (closed symbols) and an increase in tyrosine emission (open symbols). Both regions yield apparently two-state denaturation curves with an unfolding transition between 4 and 6 M urea. In both cases, unfolded state baselines are linear, but there is some small and reproducible nonlinearity of folded state baselines at low urea concentrations. Because the significance of this nonlinearity is unknown, the curves have been analyzed by fitting of a simple two-state model to the data, assuming linear baselines for both folded and unfolded states (solid lines). The resulting equilibrium parameters are listed in Table 1. Based on the analysis, the conformational stability of WT IL-1ra is estimated as 9.8±0.6 and 8.9±0.6 kcal/mol for the tryptophan and tyrosine data, respectively.

Figure 5(b) illustrates equilibrium denaturation of WT IL-1ra monitored by 1-anilinonaphthalene-8-sulfonic acid (ANS) fluorescence. In this experiment, concentrations of ANS and IL-1ra as low as 5 μM were used to decrease background fluorescence of unbound ANS and to minimize any interference of the dye with the unfolding equilibrium. The data have a complex profile with steep baseline regions. In the absence of urea, mixing the dye with the protein results in weak, but detectable ANS fluorescence. The unfolding transition region is seen as a signal decrease between 4.5 and 6 M urea due to

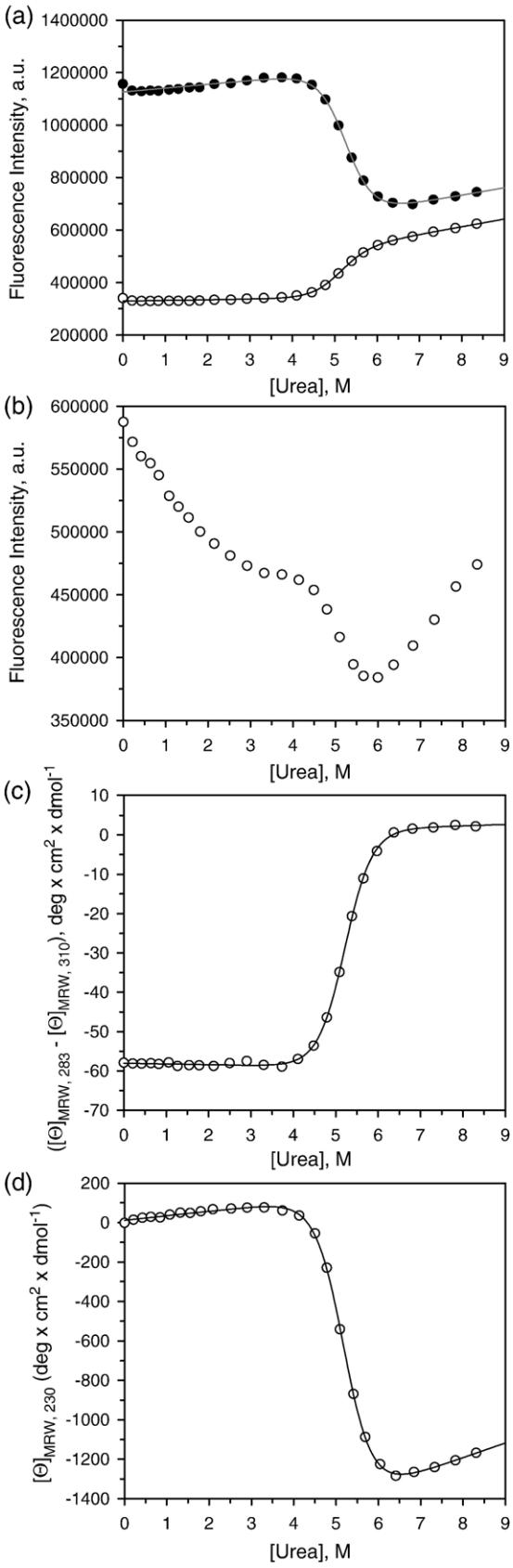

Figure 5. Equilibrium urea denaturation curves measured by (a) tryptophan (closed circles) and tyrosine fluorescence (open circles), (b) ANS fluorescence, (c) near-UV CD and (d) far-UV CD. Experimental conditions: 45 mM sodium phosphate (pH 7.0), 10% D_2O, 5 mM DTT, 5 mM HA-HCl, 25 °C. The lines represent the best fits of a two-state model to the corresponding data.

Table 1. Thermodynamic parameters by fitting of a two-state model to the urea-induced unfolding transition of WT IL-1ra monitored by near- and far-UV CD and fluorescence

Optical method	C_m (M)	m (kcal mol^{-1} M^{-1})	ΔG (kcal mol^{-1})
Trp fluorescence	5.27±0.02	1.86±0.11	9.8±0.6
Tyr fluorescence	5.09±0.03	1.75±0.11	8.9±0.6
Near-UV CD	5.22±0.01	1.86±0.05	9.7±0.3
Far-UV CD	5.19±0.01	1.77±0.03	9.2±0.2

Note. Measured at 25 °C in 45 mM sodium phosphate buffer (pH 7.0), containing 10% D_2O, 5 mM DTT, and 5 mM HA-HCl.

ANS dissociation as the protein structure unfolds. Above the transition region the signal increase is explained by urea dependence of ANS fluorescence. Overall, there is no significant ANS emission at any urea concentration. Interestingly, the initial drop in the intensity between 0 and 3 M urea is followed by a plateau at 3–4.5 M urea, prior to the unfolding transition region (see Discussion). Due to the complex character of the data and inherent ambiguity in the interpretation of ANS emission changes, no curve fitting has been attempted.

Figure 5(c) shows equilibrium denaturation of WT IL-1ra monitored by CD at 283 nm, which corresponds to one of the two negative peaks (see Figure 2(b)). To minimize the impact of baseline fluctuations, 310-nm readings were subtracted from the signal at 283 nm for every urea concentration. The resulting unfolding curve is perfectly sigmoid with nearly horizontal native and unfolded baselines. In agreement with Figure 2(b), there is a decrease in negative ellipticity as the protein unfolds. The data have been fitted based on the two-state model (solid line) and the conformational stability is estimated as 9.7±0.3 kcal/mol (Table 1).

Figure 5(d) shows equilibrium denaturation of WT IL-1ra monitored by CD at 230 nm. In agreement with Figure 2(c), protein unfolding leads to an increase in negative ellipticity: the data show a near-zero ellipticity of the folded state and ~1200 deg × cm^2 × dmol^{-1} for the unfolded state. The data have well-defined, essentially linear folded and unfolded baselines and can be fitted based on the two-state model (solid line) that yields an estimate of 9.2±0.2 kcal/mol for the conformational stability of the protein (Table 1).

Equilibrium unfolding of WT IL-1ra characterized by ^{1}H-NMR

The effect of increasing urea concentrations on IL-1ra structure has also been probed by ^{1}H-NMR. Fifteen spectra were acquired in the presence of up to 6 M urea, with 0.5 M urea increments. Figure 6 shows examples of the upfield region of the spectrum, primarily containing resonances from the methyl groups in the vicinity of aromatic residues. The methyl resonances characteristic to the native conformation are present and have constant intensities up to 4 M urea. Protein unfolding is evident from the disappearance of the resonances between 0.5 and −0.6 ppm as the urea concentration is increased above 4 M, indicating a loss of native packing interactions. The data show that IL-1ra maintains its folded conformation throughout the pretransition region between 0 and 4 M urea. However, there are some changes among the methyl resonances, for instance, at −0.2 ppm, indicating perturbation of the protein structure in response to the increase in urea. These changes are essentially complete by 2 M urea and there seem to be no substantial structural perturbations until the unfolding transition region.

Equilibrium unfolding of WT IL-1ra characterized by ^{1}H–^{15}N HSQC NMR

To obtain residue-specific information on the equilibrium denaturation mechanism of WT IL-1ra, a series of ^{1}H–^{15}N HSQC NMR spectra was recorded in the presence of up to 6 M urea, in approximately 0.5 M urea increments. Figure 7 shows the spectra measured in the presence of 0, 2.5, 4.4, and 5.2 M urea for uniformly ^{2}H–^{13}C–^{15}N-labeled wild-type IL-1ra (see details of protein preparation under Materials and Methods). At 0 M urea, the protein spectrum (Figure 7, top left) shows a set of well-dispersed peaks of the folded state. Previously reported peak assignments by Stockman et al.[40] were confirmed under the experimental conditions (see Materials and Methods). In agreement with published results, the cross-peaks for the first 10 N-terminal residues have not been observed. The first 7 to 8 N-terminal residues of IL-1ra are also missing from the known crystal structures of the protein.[31–33] Earlier we showed that the first 7 N-terminal residues of recombinant human IL-1ra can

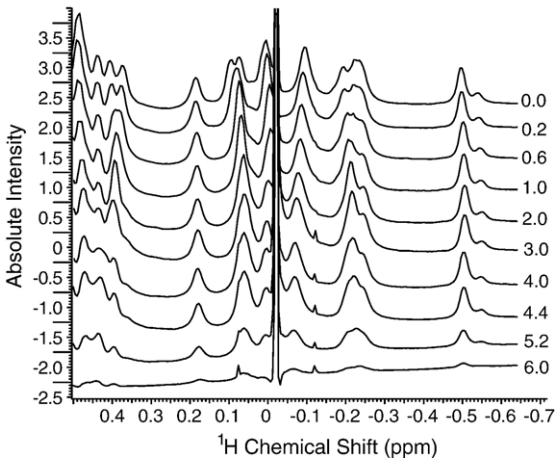

Figure 6. A stacked plot of the upfield region of 1D ^{1}H-NMR spectra for unlabeled wild-type IL-1ra measured in the presence of different molar concentrations of urea (indicated to the right). Experimental conditions: 45 mM sodium phosphate (pH 7.0), 10% D_2O, 5 mM DTT, 5 mM HA-HCl, 25 °C.

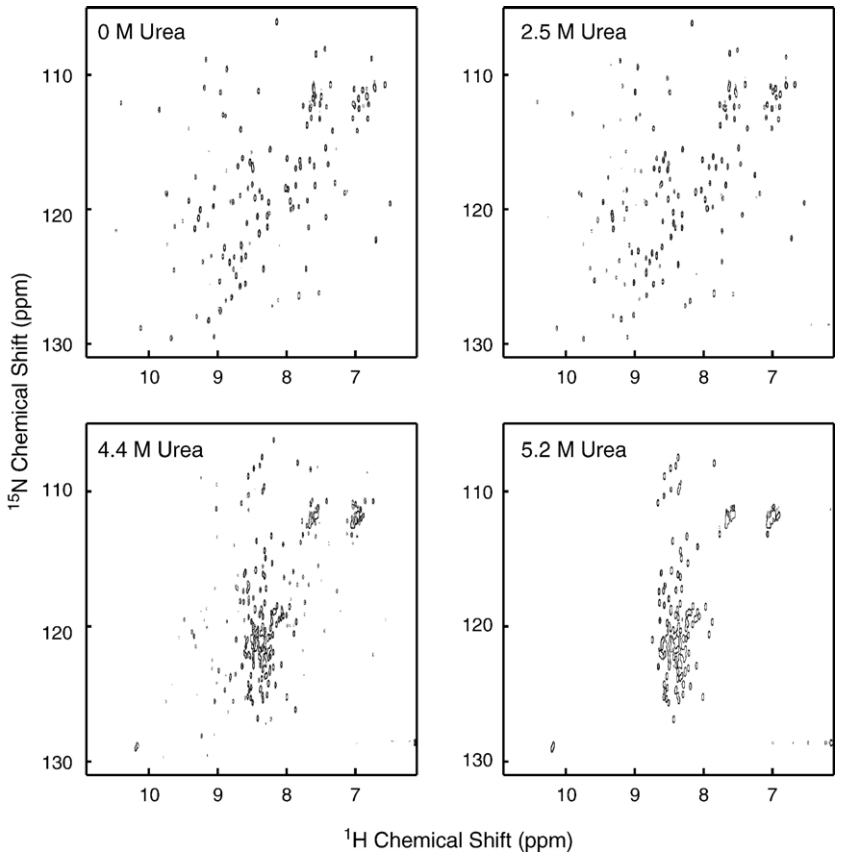

Figure 7. ^{1}H–^{15}N HSQC spectra of uniformly ^{2}H–^{13}C–^{15}N-labeled WT IL-1ra (in 45 mM sodium phosphate (pH 7.0), 10% D_2O, 5 mM DTT, and 5 mM HA-HCl) recorded at 25 °C in the absence of urea (top left) and in the presence of increasing molar concentrations of urea, as indicated.

be selectively cleaved by Lys-C protease,[34] which, together with the structural data, suggests solvent exposure and flexibility of this part of the molecule. The correlation map of IL-1ra undergoes only minor changes as the urea concentration increases from 0 to 2.5–3.0 M (cf. Figure 7, top). Further increase in urea results in the appearance of a different set of peaks originating from the denatured state. Although residue-specific assignments for unfolded IL-1ra are not available, spectral properties of the protein in 5.2 M urea (Figure 7, bottom right) are characteristic of a disordered, largely unfolded conformation. The spectrum at 4.4 M urea (Figure 7, bottom left) shows peaks originating from both folded and unfolded states in a slow conformational exchange on the NMR chemical shift timescale. In general, there are no significant chemical shift changes for the majority of the folded state resonances, except for the amide cross-peak of Leu31 that shows a pronounced urea dependence. An overlay of expanded HSQC spectra illustrating the urea-dependent shift of Leu31 is shown in Figure 8(a). In Figure 8(b) its ^{1}H chemical shift values obtained in two independent experiments are combined and plotted as a function of the denaturant concentration. Since no line broadening is evident for this peak upon urea addition, the exchange between urea-bound and unbound states is fast on the chemical shift timescale. Therefore, the shift in the peak position relative to the 0 M urea spectrum is directly proportional to the fraction of the bound state, assuming 1:1 specific binding of a single urea molecule to the protein. We have used the data for Leu31 to estimate the fraction of bound IL-1ra as a function of urea concentration, as well as the dissociation constant (K_d) for urea binding (see Materials and Methods). The fraction of bound protein plotted as a function of urea concentration and the best-fit hyperbolic curve are shown in Figure 8(c). The K_d value for the urea interaction with the amide of Leu31 is estimated as 0.95±0.04 M.

Discussion

Optical properties of Trp17 and Trp120: Implications to IL-1ra folding studies

To characterize spectral properties of individual tryptophan residues, two single tryptophan variants of IL-1ra were constructed, W17A and W120F. Both variants expressed well and showed thermal stability only slightly lower than that of the wild-type protein. However, their fluorescence and CD characteristics were different.

Emission of Trp120 is quenched as evidenced by the weak residual fluorescence of W17A compared to the wild-type protein (Figure 2(a)). Because cysteine residues are efficient quenchers of tryptophan fluorescence,[38,41] the low emission of Trp120 can be explained by the presence of two cysteines, Cys117 and Cys123, within the same chain segment. Consistent with this, emission of W17A is quenched in both folded and unfolded states. A potential disulfide

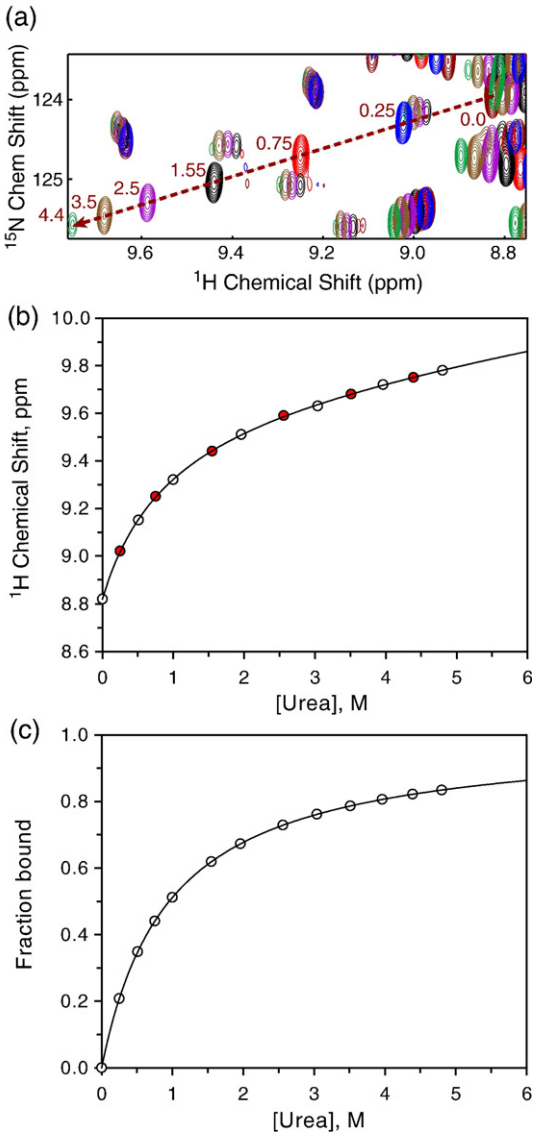

Figure 8. (a) An overlay of expanded HSQC spectra of uniformly ^{2}H–^{13}C–^{15}N-labeled WT IL-1ra for various urea concentrations. The shifting Leu31 amide cross-peak and the corresponding molar denaturant concentrations are indicated. (b) Urea-induced chemical shift changes for the Leu31 amide cross-peak in the ^{1}H dimension. Open and red symbols correspond to the data obtained in two independent experiments. The line represents the best fit of a 1:1 binding model to the combined data. (c) Fraction of urea-bound IL-1ra as a function of urea concentration.

link, Cys70–Cys117,[32] can also play a role in quenching Trp120, but this is unlikely because the experiments were performed in the presence of 5 mM DTT. However, an additional quenching interaction with Cys70 in the folded state cannot be dismissed and may explain the observed increase in W17A fluorescence upon unfolding. In contrast, Trp17 is a hyperfluorescent tryptophan residue, as seen from the comparison between folded W120F and equimolar NATA. The magnitude of the intensity drop upon denaturation and the overall intensity for W120F are close to those observed for WT IL-1ra, indicating that Trp17 is the dominant fluorescent tryptophan residue in the protein. The small decrease in the intensity of W120F compared to the wild-type protein can be explained by the removal of Trp120. Beside this, contribution of Trp120 to the emission spectrum of the protein is hardly noticeable and, therefore, fluorescence measurements of WT IL-1ra denaturation would mainly report structural perturbations in the vicinity of Trp17.

Analysis of near-UV CD characteristics of the mutant proteins shows that Trp17 and Trp120 differ in their contribution to the wild-type spectrum. The spectrum of W120F is qualitatively similar to, but twice as large as, that of WT IL-1ra. In contrast, the spectrum of W17A exhibits positive ellipticity throughout the aromatic range and is closer to the denatured spectra. Thus, the same Trp17 makes a dominant contribution to the aromatic CD spectrum. In the absence of mutation-induced structural changes one can expect additive spectral contributions, so that a sum of CD spectra of single tryptophan variants resembles that of the wild-type protein.[42] The green line in Figure 2(b) corresponds to the sum of the spectra of W17A and W120F. It can be seen that in general there is good agreement between the calculated and the wild-type spectra. Due to the high sensitivity of near-UV CD to structural changes, this technique is often used as a fingerprint of a native conformation. Therefore, this result, together with the thermal denaturation data, serves as evidence of a correctly folded conformation of W17A and W120F.

Far-UV CD analysis of the proteins also shows differences in their spectral properties (see Figure 2(c)). W120F and WT IL-1ra have qualitatively similar characteristics, while W17A is different. The folded state of the latter has a spectrum roughly intermediate between those of the folded and unfolded states of the wild-type protein. Tryptophan residues can make a significant contribution to the CD spectra of β-sheet proteins even at shorter wavelengths.[42] Because Trp17 and Trp120 have distinct near-UV CD characteristics, they may also contribute differently in the far-UV region. Along this line of reasoning, the dominance of Trp17 in the aromatic CD can explain the far-UV spectral similarity of WT and W120F, where Trp17 is present. And, therefore, CD measurements at 230 nm are expected to probe changes in both secondary and tertiary structures of the protein.

The tryptophan mutations result in only a small overall protein destabilization (see Figure 3) and the W120F substitution may be more destabilizing than W17A, even though the latter represents a dramatic reduction in side-chain volume. Based on the near-UV CD and thermal denaturation data, we argue that the single tryptophan variants of IL-1ra are suitable for characterizing individual tryptophan spectral contributions. However, because the available data do not provide explicit structural information, more studies are required to further elucidate effects of the mutations.

Mechanism of urea-induced unfolding of IL-1ra

Urea unfolding of IL-1ra is an intrinsically slow process, which resembles that of the structurally close IL-1β.[7] CD and size-exclusion HPLC experiments showed that kinetic unfolding of IL-1ra can be described as a single-exponential process with the rate constant on the order of 7.0×10^{-5} s^{-1} in 6.5 M urea at 25 °C. The close correspondence between the rate constants obtained from the near-UV CD and hydrodynamic measurements suggests that disruption of the structure around Trp17 and the global unfolding of the protein happen essentially simultaneously. Based on the HPLC data, the folded state of IL-1ra has a constant retention time throughout the course of the unfolding process. This serves as direct evidence that, even after many hours of denaturation, a fraction of molecules exhibiting a native-like compactness can be observed. No accumulation of expanded conformations is detected within the first 10 min of the reaction. The unfolded peak shows an exponential growth at the expense of the folded peak and also has a constant retention time. Although HPLC would not resolve any transient conformations rapidly exchanging with the folded and unfolded states, the data show that the remarkably slow unfolding of IL-1ra is a cooperative process characterized by a loss of protein compactness. This finding seems to contradict real-time NMR data for IL-1β, which suggested a noncooperative unfolding process for the latter.[7] Beside the fact that IL-1ra and IL-1β are two different proteins, the apparent contradiction may be explained by limitations of the techniques, with NMR and size-exclusion HPLC providing different levels of structural information. It is possible that small structural changes that may precede global unfolding of the proteins do not result in significant changes in the overall compactness and therefore remain undetected by HPLC (time-resolved NMR analysis of IL-1ra denaturation will be presented elsewhere).

The main result of the equilibrium multiparametric analysis, which included far- and near-UV CD, as well as tryptophan and tyrosine fluorescence, is illustrated in Figure 9. The unfolding data were analyzed based on the two-state model, and the denaturation curves were subsequently normalized using the fitted baseline values. There is agreement between unfolding transitions measured by different optical techniques, consistent with the two-state mechanism of protein denaturation (Table 1).[43] However, the mutant analysis shows that optical measurements of IL-1ra are strongly affected by spectral changes due to Trp17. For example, there is close similarity between the equilibrium parameters from the aromatic CD and tryptophan fluorescence data, which is not surprising because these two techniques predominantly probe structural changes around Trp17 (see above). Roughly half of the wild-type far-UV CD signal at 230 nm is contributed by Trp17 (see Figure 2(c)). It is also likely that tyrosine emission of native IL-1ra is quenched due to resonance energy transfer to Trp17, as suggested by the proximity of the tyrosine residues to the tryptophan in the crystal structure. Therefore, partial unfolding events in some other parts of the protein molecule may remain undetected. Indeed, the tyrosine data exhibit a marked deviation from linearity at low urea concentrations, suggesting some changes in the molecule in the presence of nondenaturing levels of urea (Figure 9, green triangles).

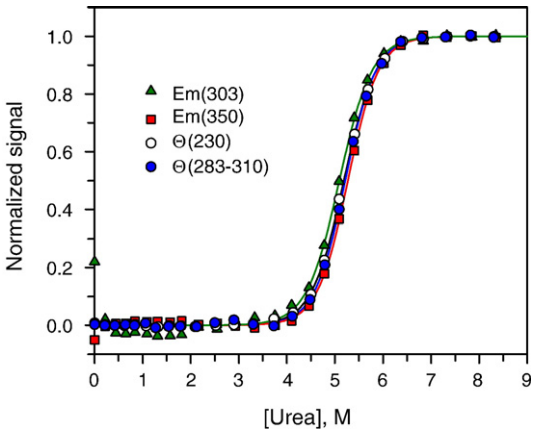

Figure 9. Normalized equilibrium urea denaturation curves measured by tyrosine fluorescence (green triangles), tryptophan fluorescence (red squares), far-UV CD (open circles), and near-UV CD (blue circles).

In order to further characterize IL-1ra denaturation we employed ANS binding and NMR. Overall, there is no substantial ANS fluorescence at any urea concentration, including the pretransition region, which argues against the accumulation of molten globule-like states.[10,43] Interestingly, the decrease in ANS signal at 0–3 M urea is followed by a plateau that precedes the unfolding transition region (see Figure 5(b)). Binding of the hydrophobic dye to the folded protein may decrease with the increase in denaturant concentration due to nonspecific effects, such as changes in bulk solvent properties, irrespective of conformational changes. This could explain the initial drop in signal intensity, but then the existence of the plateau at 3–4.5 M urea would suggest conformational changes that increase affinity of ANS to the protein. On the other hand, the complex shape of the pretransition region may also result from site-specific displacement of ANS molecules from urea-binding pockets on the surface of the protein. To further characterize this phenomenon we studied IL-1ra denaturation by ^{1}H-NMR. Close inspection of the aliphatic, aromatic, and upfield regions of the spectra reveals some structural changes when urea concentration is increased from 0 to 2 M. For instance, small changes can be seen at −0.2 ppm, indicating perturbation of the protein structure (Figure 6). At the same time, the upfield region exhibits intense resonances up to 4 M urea, suggesting no unfolding in agreement with the optical data. Further increase in urea leads to the disappearance of resonances between 0.5 and

−0.6 ppm, consistent with the loss of native packing interactions. It is yet to be seen whether the ANS and ^{1}H-NMR data report the same changes within the pretransition region and whether these changes can be attributed to specific denaturant effects. The possibility of the latter, however, seems to be supported by 2D NMR. With the exception of the amide cross-peak of Leu31, the majority of the folded peaks undergo only small chemical shift changes between 0 and 4.4 M urea (Figure 7). Within the unfolding transition region the ^{1}H–^{15}N HSQC data are consistent with only the folded and unfolded states in a slow conformational exchange on the NMR chemical shift timescale. No new cross-peaks are observed throughout the range of urea concentrations beside the ones that originate from the folded and unfolded conformations. However, individual unfolding patterns for many of the folded resonances are nonuniform in terms of peak intensity, especially between 0 and 3.5 M urea, suggesting noncooperative changes within the folded state ensemble (a more detailed analysis of the NMR data will be presented elsewhere).

Urea binding and protein denaturation studies

The estimated K_d for 1:1 urea binding to the amide of Leu31, 0.95±0.04 M, corresponds to at least a five times higher affinity than previously reported values for nonspecific interactions of proteins and peptides with urea.[44–46] This is particularly interesting because the mechanism of protein–denaturant interactions is the subject of much discussion, questioning whether it simply represents weak binding of denaturant molecules to specific protein sites[47,48] or whether it is dominated by indirect changes in solvent properties as in the transfer or linear free energy models.[49–55] The available data suggest a weak binding of urea to denatured proteins with widely varied estimates of K_d and the observed variability likely reflects the existence of multiple denaturant binding sites with different affinities characteristic of disordered conformations. In contrast, specific denaturant binding to a folded protein would likely be favored by a local protein structure. Lumb and Dobson reported urea binding to the native state of hen lysozyme,[56] where a number of denaturant molecules were implicated in binding, but the chemical shift changes were primarily associated with the substrate binding site. In the case of IL-1ra we are unaware of any functionally important ligand binding in the vicinity of Leu31. Analysis of IL-1ra crystal structures (PDB ID: 1ILR,[32] 1IRA[33]) suggests that the amide proton of Leu31 is located in a well-defined cavity forming an entrance to the interior of the β-barrel (see stereo view in Figure 10), structural properties of which apparently stabilize the protein–urea interaction. One of the crystal structures (PDB ID: 1ILR[32]) contains water molecules, which are directly hydrogen bonded to the amide of Leu31. Displacement of water molecules by urea could serve as a mechanism that explains large chemical shift changes at this particular location, while the rest of the protein structure remains essentially unperturbed.

In general, specific denaturant binding events would be difficult to observe in the absence of residue-level information provided by NMR. Nevertheless, it is important to explore whether denaturant binding can potentially induce changes in protein spectral characteristics (for instance, *via* binding in the vicinity of chromophores), because it may have implications to protein denaturation studies.

Among the β-trefoil proteins, IL-1ra and IL-1β share the highest degree of sequence similarity[29] and, as follows from this study, have similar unfolding properties. It was previously shown for IL-1β that its sole tryptophan residue (Trp120) exhibits a biphasic emission change upon denaturant titration.[2] Based on NMR data in guanidine

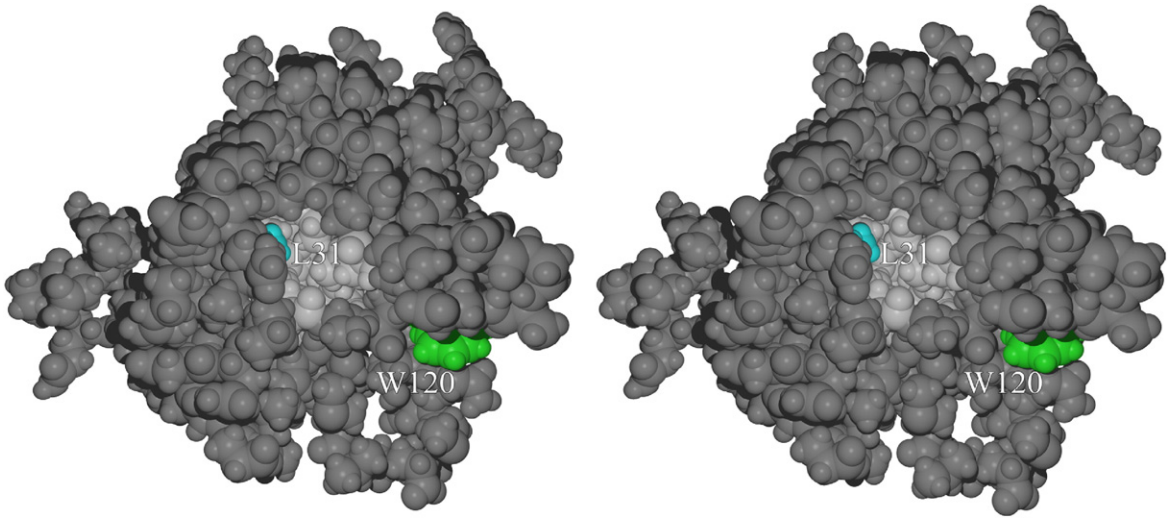

Figure 10. A wall-eye stereo image illustrating the cavity (light gray) on the surface of IL-1ra. The side-chains of Leu31 and Trp120 are shown in cyan and green, respectively. The amide of Leu31 is not visible in this representation.

hydrochloride, it was concluded that IL-1β represents the case with no populating partially unfolded states, while the biphasic behavior was attributed to the heterogeneity of its folded state ensemble.[8] IL-1ra contains an additional (hyperfluorescent) tryptophan residue, Trp17, which does not exhibit biphasic emission change upon equilibrium unfolding. Being structurally similar, IL-1β has a cavity that resembles that of IL-1ra and contains Leu26, which is equivalent to Leu31 in the receptor antagonist. Moreover, based on the crystal structure there is a water molecule that is directly hydrogen bonded to the amide of Leu26 (PDB ID: 2I1B[17]). It is, therefore, interesting to see whether urea can displace water and induce chemical shift changes in IL-1β in a fashion similar to IL-1ra and whether any correlation can be found between urea binding and protein fluorescence. As illustrated for IL-1ra in Figure 10, the urea-binding site and Trp120 are not too distant from each other and denaturant binding in a nearby region could potentially affect tryptophan fluorescence.

Materials and Methods

High-purity recombinant human (nonglycosylated) IL-1ra was supplied by an Amgen manufacturing facility. Urea was obtained from ICN Biomedicals, Inc. (Aurora, OH) (ultra pure grade). All chemicals were of reagent grade or higher quality. Unless stated otherwise, the standard conditions used for biophysical measurements were 45 mM sodium phosphate (pH 7.0), 10% D_2O, 5 mM DTT, 5 mM hydroxylamine hydrochloride (HA-HCl) (cyanate scavenger, see below), 25 °C. These conditions were chosen to ensure the same sample composition for NMR and optical measurements. Under these conditions no aggregation or nonnative disulfide formation/scrambling were observed.

Expression and purification of ^{2}H–^{13}C–^{15}N-labeled IL-1ra

The ^{2}H–^{13}C–^{15}N-labeled IL-1ra was expressed and purified as follows. The *Escherichia coli* strain GM121 (ATCC No. 202174) expressing the wild-type IL-1ra in the pAMG21 vector (ATCC No. 98113) was inoculated into 50 ml of Celtone-natural medium (Spectra Stable Isotopes, Inc., Columbia, MD) supplemented with 40 μg/ml of kanamycin. This culture was incubated at 37 °C in a 300-ml baffled Ehrlenmyer flask with shaking at 250 rpm. After 8 h the culture was centrifuged and the supernatant was discarded. The cells were resuspended in 1 l of Celtone-DCN medium from Spectra Stable Isotopes (>97% ^{2}H, >98% ^{13}C, >98% ^{15}N). Cells were grown at 37 °C in a 2800-ml Fernbach flask to an optical density of 1.0 at 600 nm and then induced with 300 μg/l of *N*-(β-ketocaproyl)-DL-homoserine lactone autoinducer (K-3255, Sigma–Aldrich Corp., St Louis, MO). The culture was incubated for an additional 14 h at 37 °C and then harvested by centrifugation. The wet cell pellet (1–2 g) was resuspended in 5 ml of cold buffer A (25 mM sodium acetate, 100 mM NaCl, 1 mM EDTA, pH 5.2) and sonicated on ice (4 pulses, 30 s each). Following centrifugation at 4 °C (12,000 rpm, 60 min) the supernatant was taken, the pellet was washed with 1.5 ml of buffer A, and the material was centrifuged again. The supernatants were combined and the solution was adjusted to pH 5.2 with 1 M acetic acid. After overnight incubation at room temperature the material was centrifuged at 10,000 rpm for 30 min. The resulting supernatant was loaded onto a GE Healthcare SP Sepharose Fast Flow column (0.7×7.5 cm) pre-equilibrated with buffer A. After the column was washed with 2 column volumes of buffer A, the ^{2}H–^{13}C–^{15}N-labeled IL-1ra was eluted with a stepwise gradient of buffer B (25 mM sodium acetate, 280 mM NaCl, 1 mM EDTA, pH 5.2). The protein fraction was analyzed by SDS–PAGE, dialyzed against buffer C (10 mM histidine, 50 mM NaCl, 0.1 mM EDTA, pH 6.0), and centrifuged (11,000 rpm, 40 min). The supernatant was loaded onto a GE Healthcare Q-Sepharose XL column (0.7×9.5 cm) pre-equilibrated in buffer C, and the flow-through fractions were collected and analyzed by SDS–PAGE. The ^{2}H–^{13}C–^{15}N-labeled IL-1ra was found in the flow-through and concentrated using an Amicon Ultracell YM5 stirred cell. The protein solution was exchanged with 25 mM sodium acetate, 1 mM EDTA, pH 5.2, and stored at −70 °C. Identity and intactness of the ^{2}H–^{13}C–^{15}N-labeled IL-1ra were verified by RP HPLC/MS Lys-C peptide mapping using unlabeled protein as a reference.

Construction, expression, and purification of single tryptophan mutants of IL-1ra

The W17A and W120F mutations were introduced into the sequence of IL-1ra in the pAMG21 vector by site-directed mutagenesis via overlapping oligonucleotides and PCR. The GM121 strain was transformed with the resulting vectors *via* electroporation and the colonies were selected on Luria broth plates supplemented with 40 μg/ml kanamycin. Cells were grown in 10-l culture volumes in 15-l Biolaffite 78 100 series fermenters in a medium containing 0.5 ml/l Fluka P2000 polyethylene glycol, 50 g/l Quest International NZ-Amine HD, 0.3 g/l sodium citrate, 4 g/l dibasic potassium phosphate, 1 g/l magnesium sulfate-heptahydrate, 2 g/l ammonium sulfate, 80 g/l glycerol, 60 μg/l biotin, 40 μg/l folic acid, 420 μg/l riboflavin, 1.4 mg/l pyridoxine hydrochloride, 6.1 mg/l niacin, 5.4 mg/l pantothenic acid, 27 mg/l ferric chloride, 2 mg/l zinc chloride, 2 mg/l cobalt chloride, 2 mg/l sodium molybdate, 1 mg/l calcium chloride, 1.9 mg/l cupric sulfate, 0.5 mg/l boric acid, 1.6 mg/l manganese chloride, and 73.5 mg/l sodium citrate dihydrate. The pH was controlled at 7.0 and dissolved oxygen was maintained at a minimum of 20% of saturation. Cells were grown at 37 °C to an optical density of 8 to 11 at 600 nm and then induced with 300 μg/l of *N*-(β-ketocaproyl)-DL-homoserine lactone and harvested by centrifugation 6 h later. The resulting wet cell pellet (~70 g) was resuspended in 10 vol (1 g/10 ml) of 10 mM sodium acetate, 50 mM NaCl, 5 mM EDTA, pH 5.2, and the cells were lysed at 16,000 psi using a microfluidizer (Model 110S, Microfluidics Corp.). The resulting lysate was centrifuged for 30 min at 10,000*g* at 4 °C. Both mutants were detected in the soluble fraction of the lysate by SDS–PAGE. The clarified lysate solution with conductivity of 10 mS/cm was applied directly to a Pharmacia SP-Sepharose (3.2×10 cm) fast flow cation exchange column equilibrated with 10 mM sodium acetate, 0.1 M NaCl, 1 mM EDTA, pH 5.2, with a flow rate of 6 ml/min, at 4 °C. The column was then washed with 5 column volumes of the equilibration buffer. A 10-column volume linear gradient from 0.1 to 0.25 M NaCl was used to elute the IL-1ra mutants. The fractions were collected and pooled based on SDS–PAGE Tris–glycine gel analysis. Subsequently, the protein

fractions were concentrated and buffer was exchanged using an Amicon S1Y3 spiral cartridge (Millipore, Inc., Billerica, MA) *versus* 10 mM histidine, 0.1 M EDTA, pH 6.2, and applied to a Pharmacia Q-hp (2.6×10 cm) anion exchange column equilibrated with 10 mM histidine, 20 mM NaCl, 0.1 M EDTA, pH 6.2, at room temperature (with a flow rate of 5 ml/min). The column was washed with 5 column volumes of the equilibration buffer. A 10-column volume linear gradient from 20 to 85 mM NaCl was used to elute the IL-1ra variants. The fractions were collected and pooled based on SDS–PAGE Tris–glycine gel analysis. Both mutant proteins were concentrated up to ~14 mg/ml and dialyzed versus 50 mM sodium phosphate buffer, pH 7.0. Identity and intactness of the W17A and W120F variants were verified by RP HPLC/MS Lys-C peptide mapping using the wild-type protein as a reference.

Suppression of IL-1ra carbamylation in urea

Mass spectral analysis of IL-1ra exposed to high concentrations of urea at pH 7 showed substantial carbamylation of the protein within a few hours at room temperature (data not shown). Because complete conformational equilibration of IL-1ra requires more than 12 h due to intrinsically slow unfolding (see Results), various cyanate scavengers were tested to suppress the unwanted modification. Comparison of Gly-Gly, ethylenediamine, and HA-HCl with the amino group p*K* values of 8.3, 7.0, and 6.2, respectively, showed that hydroxylamine is the most effective scavenger in agreement with its lower p*K*.[57] HA-HCl concentrations as low as 5–10 mM were adequate for suppressing IL-1ra carbamylation for the duration of the experiments and did not interfere with ^{1}H–^{15}N HSQC. HA-HCl concentrations such as 50 mM or higher induced multiple +16 Da modifications of the protein upon prolonged incubation, possibly due to oxidation. In this study, its concentration was kept at 5 mM and no effects on protein structure and stability were observed based on RP HPLC/MS, optical spectroscopy, and NMR.

Urea-induced unfolding experiments

Equilibrium titration experiments were performed on separately prepared protein solutions with different concentrations of urea, following an overnight incubation at 25 °C. The denaturant concentration for each point of the titration was determined by measuring refractive index ($\pm 3\times10^{-4}$) using a Leica Abbe Mark II refractometer (Leica Microsystems, Exton, PA). The wild-type IL-1ra concentration was estimated using a theoretically calculated extinction coefficient of 15,470 M^{-1} cm^{-1} at 280 nm. The single tryptophan mutant concentrations were calculated using an extinction coefficient of 9970 M^{-1} cm^{-1}.

Optical spectroscopy

Fluorescence measurements were performed on a T-format Quanta 6 PTI fluorimeter (Photon Technology International, Lawrenceville, NJ) equipped with two emission channels and a thermoelectric temperature control unit. For generating equilibrium denaturation curves, the excitation wavelength was set to 280 nm and the emission channels were set to 303 and 350 nm to allow for simultaneous detection of the tyrosine and tryptophan emission, respectively. The excitation bandwidth was set to 4 nm and the emission bandwidths were set to 10 and 6 nm for the corresponding emission channels. The signal intensity at every denaturant concentration was an average of a 60-s kinetic measurement. For spectral measurements, protein fluorescence was excited at 280 nm and scanned from 290 to 400 nm. The excitation and emission bandwidths were set to 1 and 6 nm, respectively. The spectrum of a blank buffer solution measured under identical conditions was used for subtracting the Raman peak of water. Typically, 3–8 μM protein solutions were used for the fluorescence measurements.

ANS emission was excited at 375 nm and measured at 492 nm with the excitation and emission bandwidths set to 10 and 12 nm, respectively. ANS emission intensity as a function of urea was plotted based on 10-s kinetic measurements to minimize signal decrease due to photobleaching. The dye and the protein concentrations were 5 μM.

CD measurements were performed on a Jasco J-810 spectropolarimeter (Jasco, Easton, MA) equipped with a thermoelectric temperature control unit. Urea-induced denaturation in the far-UV region was monitored at 230 nm with 0.2-cm path-length and a 3-nm bandwidth; changes in the near-UV (aromatic) region were followed at 283 and 310 nm (to account for the baseline drifts), with 1-cm path-length and a 2-nm bandwidth. Signal intensity was recorded at each denaturant concentration for 120 s and the data points were averaged to improve quality of the data. Spectral measurements including wavelengths shorter than 230 nm were performed with 0.1-cm path-length and a 4-nm bandwidth. Spectra of blank buffer solutions acquired under identical conditions were used for background correction. Steady-state spectra were recorded by scanning 215 to 260-nm and 240 to 330-nm wavelength ranges for the far- and near-UV CD, respectively. Protein concentrations were 25–80 μM and 50–80 μM for the far and near-UV CD measurements, respectively.

CD thermal denaturation measurements at 230 nm were performed as described previously.[34] Briefly, a 5 to 85 °C temperature range was monitored with the rate of temperature change of 1 °C/min, using 1-cm path-length and a 4-nm bandwidth. Reversibility of the denaturation was verified by an inverse temperature scanning immediately after the 85 °C set point was reached, with the same rate of temperature change. Protein solutions of 80 μM were incubated overnight at 25 °C in 50 mM sodium phosphate, 5 mM DTT, 5 mM HA-HCl, pH 7.0. Immediately prior to the denaturation measurements, protein solutions were diluted down to 5 μM using 45 mM sodium phosphate buffer (pH 7.0), containing 10% D_2O and 0.5 M NaCl.

NMR spectroscopy and quantitative peak shift analysis

All NMR experiments were performed at 25 °C using a Bruker DRX Avance 600 MHz NMR spectrometer (Bruker) equipped with an inverse TXI, *z*-gradient cryogenic probe.

1D ^{1}H-NMR denaturation experiments were performed using 1 mM samples of unlabeled wild-type IL-1ra. Each spectrum was acquired with 8192 complex points and signal averaged for 64 scans with eight dummy scans. Spectra were processed using the ADCLABS 1D NMR processor, referencing ^{1}H chemical shifts relative to the ^{1}H methyl resonances of DSS.

2D ^{1}H–^{15}N HSQC denaturation experiments were performed on 0.13 mM samples of uniformly ^{2}H–^{13}C–^{15}N-labeled wild-type IL-1ra. Spectra were processed using NMRPipe. ^{1}H–^{15}N HSQC experiments were run with 64 experiments in ^{15}N dimension (*t*1) consisting of 40 scans and 1024 data points in ^{1}H dimension (*t*2).

Previously published resonance assignments for wild-type IL-1ra[40] were used as a reference for reassigning the ^{1}H–^{15}N cross-peaks. HNCA, HNCOCA, and HNCACB data optimized for a deuterated protein were acquired to confirm assignments in the absence of urea, using a 0.66 mM sample of ^{2}H–^{13}C–^{15}N-labeled IL-1ra. To verify the Leu31 amide proton assignment in the presence of urea, a separate HNCACB experiment was performed using a 0.46 mM sample of ^{2}H–^{13}C–^{15}N-labeled protein in 2.5 M urea.

Quantitative peak shift analysis for Leu31, which showed a ^{1}H chemical shift change of ~1.0 ppm between 0 and 5 M urea, was performed as described by Zarrine-Afsar *et al*.[58] A linear baseline correction was required for adequate fitting of the urea binding, and the extracted correction value was 0.005 ppm/M. As suggested previously,[58] this linear dependence may reflect some small noncooperative changes of the folded state as a response to increasing concentrations of urea.

RP HPLC/MS analysis

RP HPLC/MS analysis of IL-1ra was performed on an Agilent 1100 Capillary HPLC system equipped with a UV detector, an autosampler, a nano flow cell, and a temperature-controlled column compartment (Agilent, Palo Alto, CA). The mobile phase included water with 0.1% trifluoroacetic acid (J.T. Baker, Phillipsburg, NJ) in solvent A and 70% isopropanol (Burdick & Jackson, Muskegon, MI), 20% acetonitrile (J.T. Baker), 9.9% water with 0.1% trifluoroacetic acid in solvent B. Zorbax Stable Bond SB300 C8 50×1 mm columns with 3.5-μm particle size and 300-Å pore size (Agilent and Micro-Tech Scientific, Inc., Cousteu Court, Vista) were used for RP HPLC analysis. Columns were operated at 50 °C with a flow rate of 50 μL/min. Before injection, the column was conditioned with 1% B. A linear gradient of B increasing from 30 to 45% was utilized for elution and separation of IL-1ra and its fragments generated by the limited proteolysis. The column eluate was analyzed by the UV detector and then directed to an in-line mass spectrometer. In-line with RP chromatography, electrospray ionization (ESI) time-of-flight mass spectrometry was performed on a Waters Q-Tof Micro mass spectrometer equipped with an ESI atmosphere–vacuum interface. The mass spectrometer was set to run in a positive ion mode with a capillary voltage of 3200 V, sample cone at 40 V, m/z range of 600–4000, and mass resolution of 5000. The instrument was tuned and calibrated using multiply charged ions of trypsinogen (T1143, Sigma). The deconvolution of ESI mass spectra was performed using a MaxEnt1 algorithm, which is a part of the MassLynx software from Micromass.

Size-exclusion HPLC

Size-exclusion HPLC experiments were performed on an Agilent 1100 system using Super SW 2000 column (TSK Gel, particle size 4 μm, TOSOH Bioscience) equilibrated with 6.5 M urea in 50 mM sodium phosphate (pH 7.0), 5 mM DTT, 5 mM HA-HCl, at 25 °C. The flow rate was kept at 0.3 ml/min and the pressure in the column was 100 psi. The first injection was made immediately after native IL-1ra was manually mixed with a denaturing buffer to achieve an increase in urea concentration from 0 to 6.5 M. The sample vial was kept at 25 °C in the autosampler and used throughout the course of the experiment. Snapshots of the kinetic process were obtained *via* multiple injections from the vial and by monitoring the signal at 280 nm. The chromatograms were analyzed and integrated using Chemstation software (Agilent).

Acknowledgements

We thank Jeff Lewis, Mark Michaels, and Yue-Sheng Li for their help with the construction, expression, and purification of the tryptophan variants and the uniformly ^{2}H–^{13}C–^{15}N-labeled IL-1ra; Bruce D. Mason and Edward J. Bures for their help with peptide mapping of IL-1ra samples. We also thank Janet Cheetham, Leszek Poppe and Christopher Wilde for their help with NMR experiments and data analysis. Special thanks are extended to Bruce A. Kerwin and Heinrich Roder for their expert advice and fruitful discussions. We also thank Scott Silbiger, Dan Lombardo, and Ekaterina Latypova for careful reading of the manuscript.

References

1. Murzin, A. G., Lesk, A. M. & Chothia, C. (1992). β-Trefoil fold. Patterns of structure and sequence in the Kunitz inhibitors interleukins-1β and 1α and fibroblast growth factors. *J. Mol. Biol.* **223**, 531–543.
2. Stewart, C., Schmeissner, U., Wingfield, P. & Pain, R. H. (1987). Conformation, stability, and folding of interleukin 1β. *Biochemistry*, **26**, 3570–3576.
3. Varley, P., Gronenborn, A. M., Christensen, H., Wingfield, P. T., Pain, R. H. & Clore, G. M. (1993). Kinetics of folding of the all-β sheet protein interleukin-1β. *Science*, **260**, 1110–1113.
4. Makhatadze, G. I., Clore, G. M., Gronenborn, A. M. & Privalov, P. L. (1994). Thermodynamics of unfolding of the all β-sheet protein interleukin-1β. *Biochemistry*, **33**, 9327–9332.
5. Heidary, D. K., Gross, L. A., Roy, M. & Jennings, P. A. (1997). Evidence for an obligatory intermediate in the folding of interleukin-1β. *Nature Struct. Biol.* **4**, 725–731.
6. Finke, J. M. & Jennings, P. A. (2002). Interleukin-1β folding between pH 5 and 7: experimental evidence for three-state folding behavior and robust transition state positions late in folding. *Biochemistry*, **41**, 15056–15067.
7. Roy, M. & Jennings, P. A. (2003). Real-time NMR kinetic studies provide global and residue-specific information on the non-cooperative unfolding of the β-trefoil protein, interleukin-1β. *J. Mol. Biol.* **328**, 693–703.
8. Roy, M., Chavez, L. L., Finke, J. M., Heidary, D. K., Onuchic, J. N. & Jennings, P. A. (2005). The native energy landscape for interleukin-1β. Modulation of the population ensemble through native-state topology. *J. Mol. Biol.* **348**, 335–347.
9. Samuel, D., Kumar, T. K. S., Srimathi, T., Hsieh, H. C. & Yu, C. (2000). Identification and characterization of an equilibrium intermediate in the unfolding pathway of an all β-barrel protein. *J. Biol. Chem.* **275**, 34968–34975.
10. Srimathi, T., Kumar, T. K. S., Chi, Y.-H., Chiu, I.-M. & Yu, C. (2002). Characterization of the structure and dynamics of a near-native equilibrium intermediate in

the unfolding pathway of an all β-barrel protein. *J. Biol. Chem.* **277**, 47507–47516.
11. Estape, D., van den Heuvel, J. & Rinas, U. (1998). Susceptibility towards intramolecular disufide-bond formation affects conformational stability and folding of human basic fibroblast growth factor. *Biochem. J.* **335**, 343–349.
12. Estape, D. & Rinas, U. (1999). Folding kinetics of the all-β-sheet protein human basic fibroblast growth factor, a structural homolog of interleukin-1β. *J. Biol. Chem.* **274**, 34083–34088.
13. Liu, C., Chu, D., Wideman, R. D., Houliston, R. S., Wong, H. J. & Meiering, E. M. (2001). Thermodynamics of denaturation of hisactophilin, a β-trefoil protein. *Biochemistry*, **40**, 3817–3827.
14. Liu, C., Gaspar, J. A., Wong, H. J. & Meiering, E. M. (2002). Conserved and non-conserved features of the folding pathway of hisactophilin, a β-trefoil protein. *Protein Sci.* **11**, 669–679.
15. Wong, H. J., Stathopulos, P. B., Bonner, J. M., Sawyer, M. & Meiering, E. M. (2004). Non-linear effects of temperature and urea on the thermodynamics and kinetics of folding and unfolding of hisactophilin. *J. Mol. Biol.* **344**, 1089–1107.
16. Finzel, B. C., Clancy, L. L., Holland, D. R., Muchmore, S. W., Watenpaugh, K. D. & Einspahr, H. M. (1989). Crystal structure of recombinant human interleukin-1β at 2.0 A resolution. *J. Mol. Biol.* **209**, 779–791.
17. Priestle, J. P., Schar, H. P. & Grutter, M. G. (1989). Crystallographic refinement of interleukin 1β at 2.0 A resolution. *Proc. Natl Acad. Sci. USA*, **86**, 9667–9671.
18. Clore, G. M., Wingfield, P. T. & Gronenborn, A. M. (1991). High-resolution three-dimensional structure of interleukin 1β in solution by three- and four-dimensional nuclear magnetic resonance spectroscopy. *Biochemistry*, **30**, 2315–2323.
19. Pineda-Lucena, A., Jimenez, M. A., Lozano, R. M., Nieto, J. L., Santoro, J., Rico, M. & Gimenez-Gallego, G. (1996). Three-dimesional structure of acidic fibroblast growth factor in solution: effects of binding to a heparin functional analog. *J. Mol. Biol.* **264**, 162–178.
20. Ago, H., Kitagawa, Y., Fujishima, A., Matsuura, Y. & Katsube, Y. (1991). Crystal structure of basic fibroblast growth factor at 1.6 A resolution. *J. Biochem. (Tokyo)*, **110**, 360–363.
21. Zhu, X., Komiya, H., Chirino, A., Faham, S., Fox, G. M., Arakawa, T. *et al.* (1991). Three-dimensional structures of acidic and basic fibroblast growth factors. *Science*, **251**, 90–93.
22. Habazettl, J., Gondol, D., Wiltscheck, R., Otlewski, J., Schleicher, M. & Holak, T. A. (1992). Structure of hisactophilin is similar to interleukin-1β and fibroblast growth factor. *Nature*, **359**, 855–858.
23. Chiti, F., Taddei, N., White, P. M., Bucciantini, M., Magherini, F., Stefani, M. & Dobson, C. M. (1999). Mutational analysis of acylphosphatase suggests the importance of topology and contact order in protein folding. *Nature Struct. Biol.* **6**, 1005–1009.
24. Riddle, D. S., Grantcharova, V. P., Santiago, J. V., Alm, E., Ruczinski, I. & Baker, D. (1999). Experiment and theory highlight role of native state topology in SH3 folding. *Nature Struct. Biol.* **6**, 1016–1024.
25. Clementi, C., Jennings, P. A. & Onuchic, J. N. (2000). How native-state topology affects the folding of dihydrofolate reductase and interleukin-1β. *Proc. Natl Acad. Sci. USA*, **97**, 5871–5876.
26. Chavez, L. L., Gosavi, S., Jennings, P. A. & Onuchic, J. N. (2006). Multiple routes lead to the native state in the energy landscape of the β-trefoil family. *Proc. Natl Acad. Sci. USA*, **103**, 10254–10258.
27. Dinarello, C. A. (1996). Biologic basis for interleukin-1 in disease. *Blood*, **87**, 2095–2147.
28. Watkins, L. R., Hansen, M. K., Nguyen, K. T., Lee, J. E. & Maier, S. F. (1999). Dynamic regulation of the pro-inflammatory cytokine, interleukin-1β: molecular biology for non-molecular biologists. *Life Sci.* **65**, 449–481.
29. Eisenberg, S. P., Evans, R. J., Arend, W. P., Verderber, E., Brewer, M. T., Hannum, C. H. & Thompson, R. C. (1990). Primary structure and functional expression from complementary DNA of a human interleukin-1 receptor antagonist. *Nature*, **343**, 341–346.
30. Stockman, B. J., Scahill, T. A., Strakalaitis, N. A., Brunner, D. P., Yem, A. W. & Deibel, M. R., Jr (1994). Solution structure of human interleukin-1 receptor antagonist protein. *FEBS Letters*, **349**, 79–83.
31. Vigers, G. P., Caffes, P., Evans, R. J., Thompson, R. C., Eisenberg, S. P. & Brandhuber, B. J. (1994). X-ray structure of interleukin-1 receptor antagonist at 2.0-Å resolution. *J. Biol. Chem.* **269**, 12874–12879.
32. Schreuder, H. A., Rondeau, J. M., Tardif, C., Soffientini, A., Sarubbi, E., Akeson, A. *et al.* (1995). Refined crystal structure of the interleukin-1 receptor antagonist. Presence of a disulfide link and a *cis*-proline. *Eur. J. Biochem.* **227**, 838–847.
33. Schreuder, H., Tardif, C., Trump-Kallmeyer, S., Soffientini, A., Sarubbi, E., Akeson, A. *et al.* (1997). A new cytokine-receptor binding mode revealed by the crystal structure of the IL-1 receptor with an antagonist. *Nature*, **386**, 194–200.
34. Raibekas, A. A., Bures, E. J., Siska, C. C., Kohno, T., Latypov, R. F. & Kerwin, B. A. (2005). Anion binding and controlled aggregation of human interleukin-1 receptor antagonist. *Biochemistry*, **44**, 9871–9879.
35. Heidary, D. K. & Jennings, P. A. (2002). Three topologically equivalent core residues affect the transition state ensemble in a protein folding reaction. *J. Mol. Biol.* **316**, 789–798.
36. Dougherty, D. A. (1996). Cation–pi interactions in chemistry and biology: a new view of benzene, Phe, Tyr, and Trp. *Science*, **271**, 163–168.
37. Gallivan, J. P. & Dougherty, D. A. (1999). Cation–pi interactions in structural biology. *Proc. Natl Acad. Sci. USA*, **96**, 9459–9464.
38. Lakowicz, J. R. (1999). *Principles of Fluorescence Spectroscopy*, 2nd edit., Kluwer Academic/Plenum Publishers, New York.
39. Craig, S., Pain, R. H., Schmeissner, U., Virden, R. & Wingfield, P. T. (1989). Determination of the contributions of individual aromatic residues to the CD spectrum of IL-1β using site directed mutagenesis. *Int. J. Peptide Protein Res.* **33**, 256–262.
40. Stockman, B. J., Scahill, T. A., Roy, M., Ulrich, E. L., Strakalaitis, N. A., Brunner, D. P. *et al.* (1992). Secondary structure and topology of interleukin-1 receptor antagonist protein determined by heteronuclear three-dimensional NMR spectroscopy. *Biochemistry*, **31**, 5237–5245.
41. Chen, Y. & Barkley, M. D. (1998). Toward understanding tryptophan fluorescence in proteins. *Biochemistry*, **37**, 9976–9982.
42. Freskgard, P.-O., Martensson, L.-G., Jonasson, P., Jonsson, B.-H. & Carlsson, U. (1994). Assignment of the contribution of the tryptophan residues to the circular dichroism spectrum of human carbonic anhydrase II. *Biochemistry*, **33**, 14281–14288.
43. Ptitsyn, O. B. (1995). Molten globule and protein folding. *Adv. Protein Chem.* **47**, 83–229.

44. Makhatadze, G. I. & Privalov, P. L. (1992). Protein interactions with urea and guanidinium chloride. A calorimetric study. *J. Mol. Biol.* **226**, 491–505.
45. Moglich, A., Krieger, F. & Kiefhaber, T. (2005). Molecular basis for the effect of urea and guanidinium chloride on the dynamics of unfolded polypeptide chains. *J. Mol. Biol.* **345**, 153–162.
46. Halle, B., Denisov, V. P., Modig, K. & Davidovic, M. (2005). Protein conformational transitions as seen from the solvent: magnetic relaxation dispersion studies of water, co-solvent, and denaturant interactions with nonnative proteins. In *The Protein Folding Handbook* (Buchner, J. & Kiefhaber, T., eds), pp. 201–246, Wiley-VCH, Weinheim.
47. Schellman, J. A. (1955). The stability of hydrogen-bonded peptide structures in aqueous solution. *Compt. Rend. Trav. Lab. Carlsberg*, **29**, 230–259.
48. Tanford, C. (1970). Protein denaturation. C. Part, Theoretical models for the mechanism of denaturation. *Adv. Protein Chem.* **24**, 1–95.
49. Nozaki, Y. & Tanford, C. (1963). The solubility of amino acids and related compounds in aqueous urea solutions. *J. Biol. Chem.* **238**, 4074–4081.
50. Nozaki, Y. & Tanford, C. (1970). The solubility of amino acids, diglycine, and triglycine in aqueous guanidine hydrochloride solutions. *J. Biol. Chem.* **245**, 1648–1652.
51. Schellman, J. A. (1987). Selective binding and solvent denaturation. *Biopolymers*, **26**, 549–559.
52. Schellman, J. A. (1987). The thermodynamic stability of proteins. *Annu. Rev. Biophys. Chem.* **16**, 115–137.
53. Schellman, J. A. (1990). A simple model for solvation in mixed solvents. Applications to the stabilization and destabilization of macromolecular structures. *Biophys. Chem.* **37**, 121–140.
54. Pace, C. N. (1986). Determination and analysis of urea and guanidine hydrochloride denaturation curves. *Methods Enzymol.* **131**, 266–280.
55. Pace, C. N. (1990). Conformational stability of globular proteins. *Trends Biochem. Sci.* **15**, 14–17.
56. Lumb, K. J. & Dobson, C. M. (1992). ^{1}H nuclear magnetic resonance studies of the interaction of urea with hen lysozyme. Origins of the conformational change induced in hen lysozyme by *N*-acetylglucosamine oligosaccharides. *J. Mol. Biol.* **227**, 9–14.
57. Dawson, R. M. C., Elliott, D. C., Elliott, W. H. & Jones, K. M. (2002). *Data for Biochemical Research*, 3rd edit. Oxford University Press, New York.
58. Zarrine-Afsar, A., Mittermaier, A., Kay, L. E. & Davidson, A. R. (2006). Protein stabilization by specific binding of guanidinium to a functional arginine-binding surface on an SH3 domain. *Protein Sci.* **15**, 162–170.

Edited by K. Kuwajima

(Received 13 October 2006; received in revised form 8 February 2007; accepted 9 February 2007)
Available online 22 February 2007